Journal of Thermal Analysis and Calorimetry (2019) 138:387–396
https://doi.org/10.1007/s10973-019-08219-3

Thermal degradation and flame retardancy of flexible polyvinyl chloride containing solid superacid

Ming Gao[1] · Mei Wan[2] · Xuan Zhou[1]

Received: 9 November 2018 / Accepted: 22 March 2019 / Published online: 2 April 2019

Abstract

The objective of the present article was to study the thermal degradation behavior and flame retardancy of flexible polyvinyl chloride (PVC) composites containing TiO_2/SO_4^{2-} solid superacid because of its strong catalytic ability for esterification and dehydration. The TiO_2/SO_4^{2-} solid superacid was synthesized by using precipitation immersion method, and its structure was investigated by X-ray diffraction. As expected, the value of limiting oxygen index for PVC/Sb_2O_3/(TiO_2/SO_4^{2-}) composite was 32.5% and the char yield of PVC/Sb_2O_3/(TiO_2/SO_4^{2-}) composite was significantly improved compared to neat PVC in thermogravimetry tests. In addition, the peak heat release rate and smoke production rate of PVC/Sb_2O_3/(TiO_2/SO_4^{2-}) decreased by 14% and 42%, respectively, compared with neat PVC. Moreover, the results of cone calorimetry tests and electron micrograph of char residue showed that the char yield of TiO_2/SO_4^{2-} was enhanced, resulting in a strong char layer structure with outstanding fire retardance cone. In conclusion, the results of this work showed that the addition of solid superacid promoted the decomposition and dehydration of PVC, which formed a compact and continuous char layer on the surface of the material. Hence, the study provides a new perspective for producing composites with excellent flame retardancy and smoke suppression properties of PVC.

Keywords Flame retardance · Polyvinyl chloride (PVC) · Solid superacid · Thermal degradation · Smoke suppression · Cone calorimeter

Introduction

Polyvinyl chloride (PVC) has numerous applications in industry, agriculture, communication, transportation, and construction fields, e.g., flooring, rigid pipes, flexible hoses, conveyor belts, wires, and cable insulation [1]. Due to the high content of chlorine (56.7%) in the backbone, pristine PVC has excellent flame retardancy intrinsically with LOI of 47%. Therefore, addition of flame-retardant or smoke-suppressant additives to PVC is not required [2]. However, for many applications, it is necessary to add varying amounts of an organic plasticizer, such as dioctyl phthalate (DOP), to make the PVC materials flexible and easy to process. When flexible PVC composites contain 40 parts of DOP, the LOI decreases to 26% and the material becomes highly flammable. This can cause a serious fire disaster [3]. Therefore, flame retardants are usually needed for flexible PVC in order to reduce the fire hazard [4].

In recent years, concerns have been widely expressed about the inherent toxicity of halogen flame retardants and their persistence in the environment [2]. Antimony trioxide (Sb_2O_3) is a traditional flame retardant for flexible PVC in industry. However, antimony is a toxic element that is harmful for human health. Moreover, under combustion conditions, antimony compounds produce toxic or irritating vapors. Micro amounts of antimony will stimulate respiratory tract, mucous membrane of alimentary canal and skin, and even lead to pulmonary edema or hepatomegaly [5]. Furthermore, the toxicity of Sb_2O_3 also influences environment after dissolving in soil and impairs plant growth and nitrification at certain concentrations [6].

✉ Ming Gao
gmscy@hotmail.com

[1] School of Environmental Engineering, North China Institute of Science and Technology, Box 206, Yanjiao, Beijing 101601, China

[2] School of Safety Engineering, North China Institute of Science and Technology, Box 206, Yanjiao, Beijing 101601, China

Therefore, it is important to look for a suitable alternative to Sb_2O_3. Many scholars have studied the synergistic effects of Sb_2O_3 in order to substitute part or all of it. In recent years, Pan et al. [7] proposed the mechanism of synergistic effect of nano zinc carbonate and Sb_2O_3 flame retardants added to flexible PVC. Lu et al. [8] studied the incorporation of magnesium hydroxide whiskers and magnesium hydroxide particles in PVC matrix for the complete substitution of flame retardant. Zhang et al. [9] reported that melamine–formaldehyde resin/magnesium dihydroxide/zinc stannate microcapsule had good flame retardancy and smoke suppression properties. Pi et al. [10] demonstrated the flame retardant properties of PVC containing zinc borate and zinc borate–aluminum trihydrate.

It is well known that solid superacids are effective catalysts for esterification reaction because they promote dehydration and cross-linking. Ropero-Vega et al. [11] verified that sulfated titania prepared by incipient impregnation with ammonium sulfate was an effective catalyst with very high esterification activity. Previous studies have shown that the pyrolysis of polymers includes dehydration, cross-linking, and esterification reactions [12]. Hence, in theory, solid superacids can catalyze the pyrolysis of polymers and probably act as a flame retardant. There are few reports about superacid as flame retardant. Ding et al. [13] added solid superacids to IFR/EVA composites to increase the char yields. The intumescent flame retardant system of RTB-IFR without synergistic agents mixed with modified zeolites by solid acid as flame retardant in PP system [14]. Until now, there is no relevant report on addition of solid superacid to flexible PVC as flame retardant. Consequently, in this article, an attempt to replace part of harmful Sb_2O_3 in flame-retardant PVC composites by using solid superacid was studied. The synergistic effect between solid superacid and Sb_2O_3 on the flame retardancy of flexible PVC composites was discussed. Thermal stability, flame retardancy, and carbonification of flexible PVC composites were investigated. Furthermore, the mechanism of synergistic effect of solid superacid and Sb_2O_3 in flame-retarding flexible PVC was proposed.

Experimental

Materials

Titanium tetrachloride ($TiCl_4$, 99% AR) was purchased from Shanghai McLean Technology Co., Ltd. Sulfuric acid (H_2SO_4, AR) and ammonium hydroxide were provided by Tianjin Fuchen Chemical Reagent Factory. Polyvinyl chloride (PVC) was supplied by Beijing Chemical Second Factory. Lead sulfate tribasic, dibasic lead phosphite, calcium stearate, and antimonous oxide (Sb_2O_3) were purchased from Beijing Yili Fine Chemicals Co., Ltd. Dioctyl phthalate (DOP) was obtained from Shanghai Dongfang Chemical Factory.

Synthesis of solid superacid

For the preparation of solid superacid, 30 mL of $TiCl_4$ was slowly added to distilled water in a three-necked flask with stirring at room temperature. The precursor was prepared by adding ammonia water to the above mixture with vigorous stirring until the pH was 8–10 and then aging the mixture for 24 h. The obtained precipitate was washed several times with deionized water and filtered by pump until Cl could not be detected in the filtrate. The cake after filtration was dried at 50 °C for 12 h. Then, it was impregnated with 1.3 mol L^{-1} sulfuric acid solution for 6 h and then dried by air. The obtained precipitate was sieved into 200 mesh powder and calcined in a muffle furnace at 600 °C for 2 h to obtain TiO_2/SO_4^{2-} [15].

Preparation of PVC material

The compositions of the PVC composites are given in Table 1. In a typical procedure, 100 phr PVC resin, 40 parts dioctyl phthalate (DOP), 2 phr stabilizers (lead sulfate tribasic and dibasic lead phosphite, respectively) each, 0.5 phr lubricant (calcium stearate), and 6 phr based on the total mass of flame retardant (represented by solid superacid and antimonous oxide) were dry-blended well. PVC composites were blended in a two-roll mill at 150–160 °C for 10 min, and then, the composites were introduced into a flat vulcanizing machine for compression at 165 °C and 12 MPa for 6 min. The sheets were formed after compression. Composite samples for testing were cut from the molded PVC sheet after a certain amount of time.

Table 1 Composition and LOI values of PVC composites

	PVC-0	PVC-1	PVC-2
PVC/g	100	100	100
DOP/g	40	40	40
$Pb_4O_3(SO_4)$/g	2	2	2
$2PbO{\cdot}PbHPO_3{\cdot}1/2H_2O$/g	2	2	2
$CH_3(CH_2)_{16}COO_2Ca$/g	0.5	0.5	0.5
Sb_2O_3/g	–	6	5
TiO_2/SO_4^{2-}/g	–	–	1
LOI	26.3	31.8	32.5

Characterization and analysis

X-ray diffraction (XRD)

XRD measurements were used to characterize TiO_2/SO_4^{3-} using a D/Max-3c X-ray diffractometer (D8-ADVANCE, Bruker) with Cu-Kα radiation ($\lambda = 1.54$ Å, 40 kV, 50 mA). The diffraction angle was measured over the 2θ range from 10° to 90° in steps of 1.2° for 1 min.

Limiting oxygen index (LOI)

The LOI values were measured on a JF-3 LOI apparatus (Nanjing Jiangning Analytical Instrument Co., Ltd., China). The size of each specimen was $100 \times 10 \times 3$ mm^3 according to ASTM D 2863-97. Each specimen was prepared four phr, and the measurement was repeated three times.

Thermogravimetric analysis (TGA)

TGA was conducted using a HCT-2 thermal analyzer (Beijing Hengjiu Scientific Instrument Factory) at a heating rate of 10 °C min^{-1} under nitrogen atmosphere. The mass of each sample was 7–9 mg. The range of temperature was from 25 to 700 °C.

Fourier-transform infrared (FTIR) spectroscopy

About 8 mg of each PVC compound was heated from 200 to 700 °C at a heating rate of 15 °C min^{-1} under N_2. Then, the PVC residues at different temperatures were analyzed by FTS 2000 FTIR (Varian) spectrometer with KBr powder. The FTIR spectra were recorded over the range of 4000–400 cm^{-1}.

Cone calorimeter test (CCT)

CCT was performed using a PX-07-007 system (Phoenix quality inspection instrument Co., Ltd) under an external heat flux of 50 kW m^{-2}. The specimen size was $100 \times 100 \times 3$ mm^3 according to ISO5660.

Scanning electron microscopy (SEM)

SEM micrographs of the surface of residue char layer after the CCT test were obtained by KYKYEM-3200 (China). All the samples were covered with gold before observation.

Results and discussion

X-ray diffraction (XRD)

Phase identification of the prepared catalysts was performed by XRD, as shown in Fig. 1. XRD analysis revealed that TiO_2/SO_4^{2-} influenced the crystal structure of TiO_2. According to the PDF cards, TiO_2/SO_4^{2-} exhibited intense diffraction lines at $2\theta = 25.3°$ (101), 37.8° (004), 48.0° (200), 55.07° (211), 62.6° (204), 70.3° (220), 75.1° (215), and 82.7° (224), respectively, which were all in good agreement with JCPDS-21-1272 [16]. Moreover, the peaks at $2\theta = 27.5°$ (110), 36.1° (103), 41.3°, 44.1°, and 54.3° (105) indicated the existence of the rutile state of TiO_2. Therefore, it can be inferred that TiO_2/SO_4^{2-} was a mixture of anatase and rutile TiO_2. The decrease in the crystalline size of TiO_2 due to higher FWHM of TiO_2/SO_4^{2-} peaks implied that TiO_2/SO_4^{2-} possessed the strength of the crystalline phase, strong acidity, and the ability to act on the material [17]. Some researchers [18] also mentioned that a mixture of anatase and rutile TiO_2 could show better catalytic performance. The possible reason was that the anatase crystal combined well with a small amount of rutile phase [19].

Limiting oxygen index (LOI)

LOI is defined as the minimum percentage of oxygen in an oxygen–nitrogen mixture that is sufficient to sustain combustion of the composites after ignition. LOI test is widely used to evaluate the flame retardant properties of materials [20].

The LOI values of neat PVC (PVC-0), PVC/Sb_2O_3 (PVC-1), and PVC/Sb_2O_3/(TiO_2/SO_4^{2-}) (PVC-2) samples are shown in Table 1. The LOI value of neat PVC was only 26.3%, indicating its poor flame retardant property. Compared with PVC-0, the addition of Sb_2O_3 greatly improved the flame retardant performance of PVC. The LOI value of

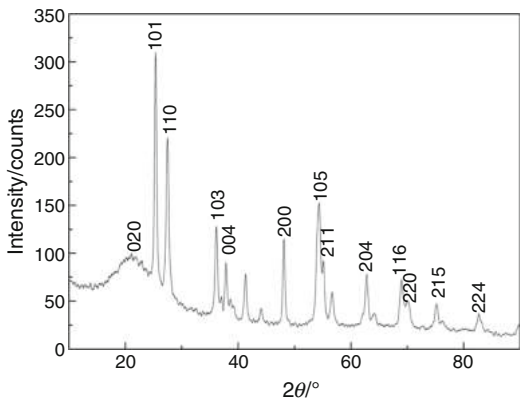

Fig. 1 XRD patterns of TiO_2–SO_4^{2-}

PVC/Sb_2O_3 was significantly improved to 31.8%. The PVC/Sb_2O_3/(TiO_2/SO_4^{2-}) composite displayed the highest LOI value of 32.3% among all PVC composites, as shown in Fig. 2. Therefore, TiO_2/SO_4^{2-} had a good synergistic effect with Sb_2O_3 in PVC.

Cone calorimeter test (CCT)

The CCT based on oxygen consumption principle can be used to compare the combustion behaviors of flame-retardant polymers efficiently [21]. The cone calorimeter is also an effective bench-scale apparatus to simulate fires [22]. Figures 2–5 show the curves of the heat release rate (HRR), total heat released (THR), the smoke production rate (SPR), total smoke produced (TSP), CO yield profile, and mass loss rate of neat PVC, PVC/Sb_2O_3, and PVC/Sb_2O_3/(TiO_2/SO_4^{2-}) composites. The detailed data are listed in Table 2.

As shown in Fig. 2a, the heat release rate (HRR) curve for neat PVC (PVC-0) exhibited a broad peak. Heat began to be released from the composites after irradiation. With increase in time, the HRR gradually increased and reached a peak value (PHRR) of 288.37 kW m^{-2} at 75 s, followed by a gradual reduction. The HRR value was close to zero after 350 s, indicating that the basic burning of neat PVC was completed [23]. The THR of neat PVC increased to the maximum of 50 kW m^{-2} in Fig. 3b. Compared to neat PVC, the HRR curves of PVC-1 and PVC-2 composite in Fig. 3a showed that the peak HRR was reduced significantly. Their THR was lower than that of neat PVC in Fig. 2b, and their TTI (time to ignition) did not change significantly. For example, the PHRR of PVC/Sb_2O_3 composites was 257.46 kW m^{-2} at 75 s and the THR was 45.2 kW m^{-2}. In particular, the PHRR of PVC/Sb_2O_3/(TiO_2/SO_4^{2-}) was 247.22 kW m^{-2} at 60 s, while the THR was 44.7 kW m^{-2}. These results suggest that TiO_2/SO_4^{2-} and Sb_2O_3 had good synergistic effect on reducing heat release. Furthermore, the insulating char layer was likely to be formed on the surface of PVC matrix during burning process. The solid superacid did not only inhibit the entry of heat and oxygen into the PVC bulk but also inhibited the exit of combustion gases out of the PVC bulk. Consequently, the intensity of combustion pyrolysis reactions reduced, and the quantity of released heat decreased too. Better understanding can be gained by analyzing the pyrolysis products from thermal decomposition [23].

In PVC composites, smoke production is usually the most important concern. Therefore, the reduction in smoke volume is a significant factor. As shown in Fig. 3a, b and Table 2, the smoke production rate (SPR), total smoke produced (TSP), and the peak SPR (PSPR) of the flame-retardant PVC all decreased compared to the corresponding values for neat PVC. At first, the TSP of neat PVC increased to the maximum of 33.4 m^2 s^{-2}, as shown in

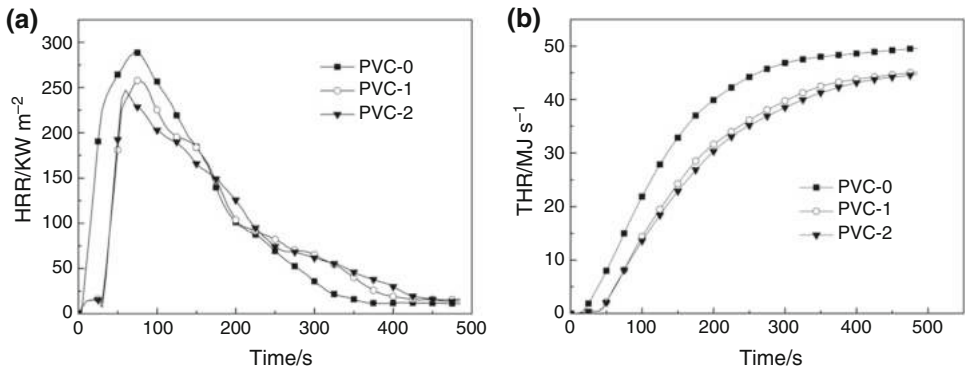

Fig. 2 HRR (**a**) and THR (**b**) curves of PVC composites

Table 2 Cone test data of PVC composites

Parameter	PVC	PVC/Sb_2O_3	PVC/Sb_2O_3/(TiO_2/SO_4^{2-})
Time to ignition/s	15	13	14
PHRR/kW m^{-2}	288	257	247
Time to PHRR/s	75	75	60
THR/kW m^{-2}	50	45	44
Peak SPR/m^2 s^{-2}	0.19	0.11	0.11
TSP/m^2 s^{-2}	33	26	27
CO yield (10^{-4})/%	2	3	5
CO_2 yield (10^{-3})/ %	6	9	8

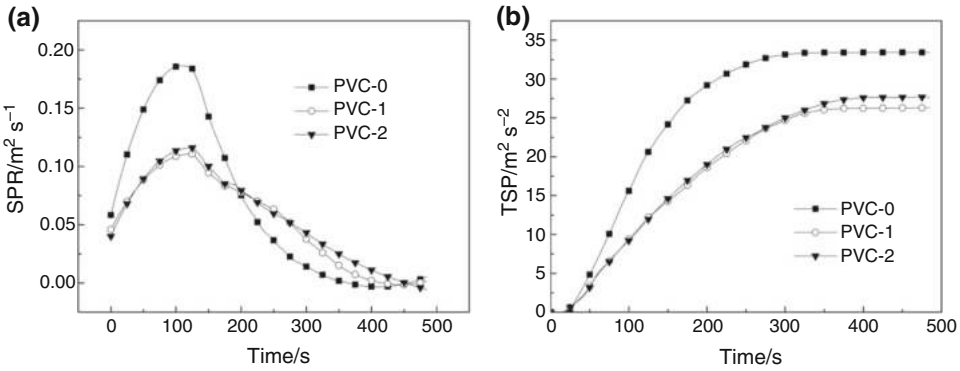

Fig. 3 SPR (**a**) and TSP (**b**) rate curves of PVC composites

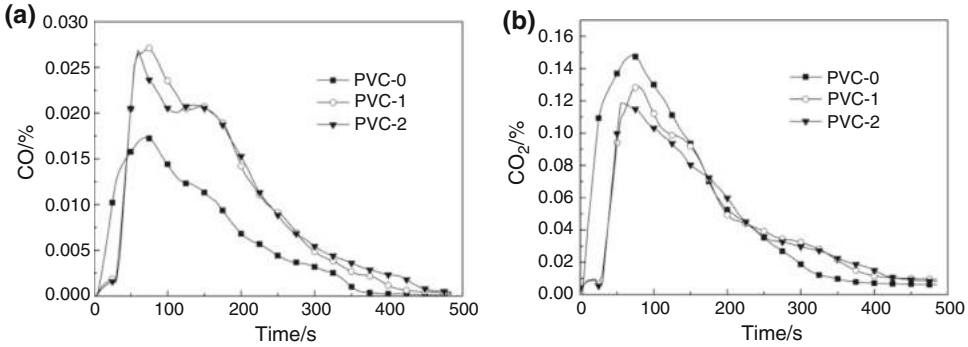

Fig. 4 CO (**a**) and CO_2 (**b**) rate curves of PVC composites

Fig. 4b. The TSP of TiO_2/SO_4^{2-} was lower than that of neat PVC by 19%, which demonstrates that TiO_2/SO_4^{2-} had a positive effect on smoke suppression of PVC. The PSPR values of the materials followed the order of: PVC (0.19 $m^2\ s^{-2}$) > PVC/Sb_2O_3 (0.11 $m^2\ s^{-2}$) ≥ PVC/Sb_2O_3/(TiO_2/SO_4^{2-}) (0.11 $m^2\ s^{-2}$), which is consistent with the data of HRR and THR. The PSPR of Sb_2O_3 was lower than that of neat PVC by 42% and was equal to that of Sb_2O_3/(TiO_2/SO_4^{2-}).

The release of poisonous gas is important for understanding the fire hazard related to materials. The toxicity of gaseous products from the combustion of materials is due to the emission of CO and CO_2 [24]. Therefore, the production of CO and CO_2 is also an important parameter for evaluating flame retardancy and flammability of polymeric materials. Figure 4a, b and Table 2 present the data for the production of CO and CO_2 for all composites. It can be seen that the CO_2 content of neat PVC soon reached the peak, which was the highest among all samples, while the CO content of neat PVC was the lowest. This is because neat PVC burns completely and releases a large amount of CO_2 gas during thermal decomposition, which indicates that it is inflammable. In the case of PVC-1 and PVC-2, the CO production was significantly increased, due to incomplete burning. Among the different composites, PVC/Sb_2O_3/(TiO_2/SO_4^{2-}) displayed lower toxic gas production, which is favorable for its fire retardant performance [25].

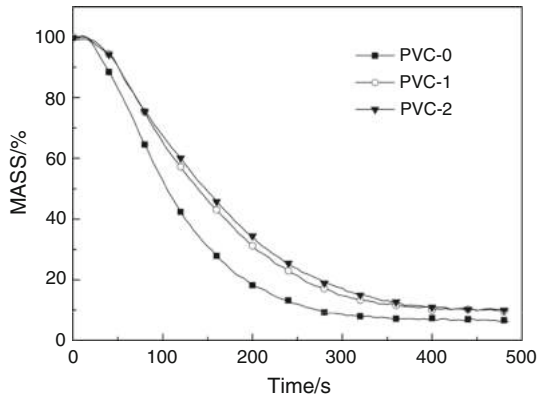

Fig. 5 MASS yield profile curves of the PVC composites

Figure 5 shows the mass loss as a function of combustion time. The increase in char residue amount of PVC-1 and PVC-2 compared with that of PVC-0 was consistent with the results in the LOI test, thus demonstrating that solid superacid and Sb_2O_3 promoted the early cross-linking of PVC to form char layer. This limited the heat and mass exchange between gas and solid phases. As a result, the flame retardant property was improved [8].

Based on the above results, it is evident that the flame retardant performance and smoke suppression property of PVC can be improved by the synergistic effect of TiO_2/SO_4^{2-} and Sb_2O_3.

Thermogravimetric analysis (TGA)

Thermogravimetry (TG) is a thermal analysis method in which the quality of a material is measured as a function of temperature. TG curve with quality percentage (or %) as the ordinate from top to bottom in turn decreases, and TG curve with temperature as the abscissa from left to right increases. The temperature or time differential first-order differential DTG curve can be obtained from the TG curve [26].

According to Figs. 6–8, the thermal degradation kinetics of all PVC compounds was studied by the Kissinger equation [27], which is as follows:

$$-\frac{E_a}{R}=\frac{d\ln\left(\Phi/T_m^2\right)}{d\left(1/T_m\right)},$$

where Φ is the rate of temperature increase in K min^{-1} (Φ = 5, 10, 15, 20); T_m is the maximum temperature at the peak position in K; R is the gas constant (8.314 J (mol K) $^{-1}$), and E_a is the decomposition activation energy. From the slope of the plot of ln ($1/T_m^2$) versus $1/T_m$, the activation energy can be calculated, i.e., $E_a = -R \times$ slope [28]. As shown in Table 3, Ea of neat PVC was 107.02 kJ mol^{-1}, and it increased by 32.73–139.75 kJ mol^{-1} when Sb_2O_3 was added to the PVC composites. Thus, it is evident that Sb_2O_3 can efficiently improve the thermal stability of PVC. For PVC/Sb_2O_3/(TiO_2/SO_4^{2-}), the Ea was 124.89 kJ mol^{-1}, which indicates that TiO_2/SO_4^{2-} catalyzed the pyrolysis of PVC composites. Consequently, the reaction energy was reduced and the PVC composites thermally degraded earlier.

Thermogravimetric analysis results (TG and DTG curves) of the PVC composite system in nitrogen atmosphere from ambient temperature up to 700 °C are shown in Figs. 6–8, and the calculated data are listed in Table 3. The temperature at which 5.0% degradation occurs is defined as the initial decomposition temperature (T_i), and the temperature at which the degradation rate reaches a maximum is defined as T_{max} [10]. It can be seen that the T_i and T_{max1} values of PVC/Sb_2O_3 were lower compared with neat PVC. Moreover, it was found that PVC/Sb_2O_3 and PVC/Sb_2O_3/(TiO_2/SO_4^{2-}) had similar values of T_i and T_{max}. Also, the T_{max2} value was higher than that of neat PVC, indicating that TiO_2/SO_4^{2-} solid superacid could catalyze pyrolysis earlier.

According to the relevant literature reports, the thermal degradation of PVC can be divided into two or more stages [29–31]. As can be seen from Figs. 6–8a, the TG curve of the composites was roughly divided into two stages of

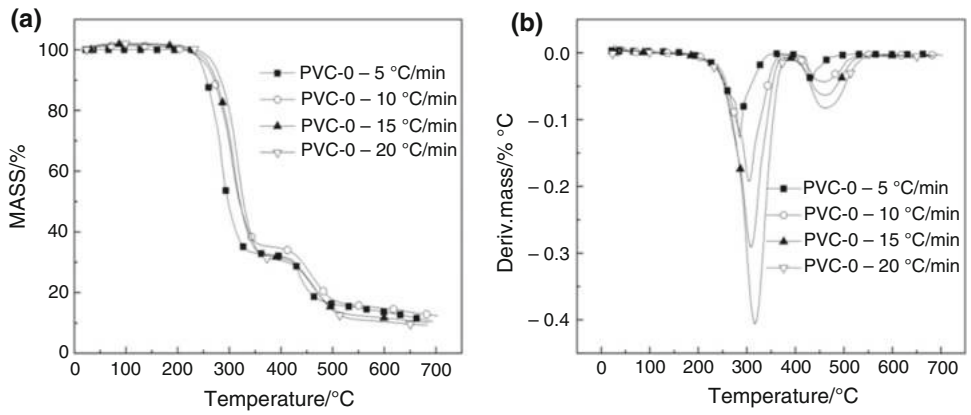

Fig. 6 TG (**a**) and DTG (**b**) curves of neat PVC at different heating rates

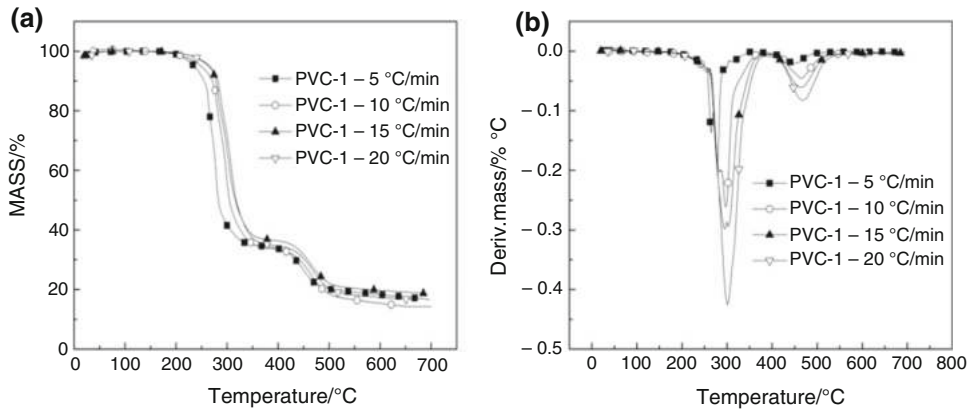

Fig. 7 TG (**a**) and DTG (**b**) curves of PVC–Sb_2O_3 at different heating rates

Table 3 Thermogravimetric analysis data of PVC composites under neat nitrogen

Sample	Φ/K min^{-1}	First step			Second step		*Ea*/kJ mol^{-1}
		T_i/°C	T_{max}/°C	Residue/%	T_{max}/°C	Residue/%	
PVC	5	247	285	33	440	10.5	107.02
	10	256	304	35	461	12.3	
	15	261	310	32	464	10.1	
	20	270	316	31	463	9.1	
PVC/Sb_2O_3	5	241	278	35	453	17.7	139.75
	10	249	296	34	465	14.3	
	15	270	295	37	464	20.2	
	20	272	300	35	468	17.8	
PVC/Sb_2O_3/(TiO_2/SO_4^{2-})	5	238	279	37	452	20.1	124.89
	10	254	297	39	464	19.8	
	15	264	303	36	466	16.9	
	20	275	304	38	469	19.8	

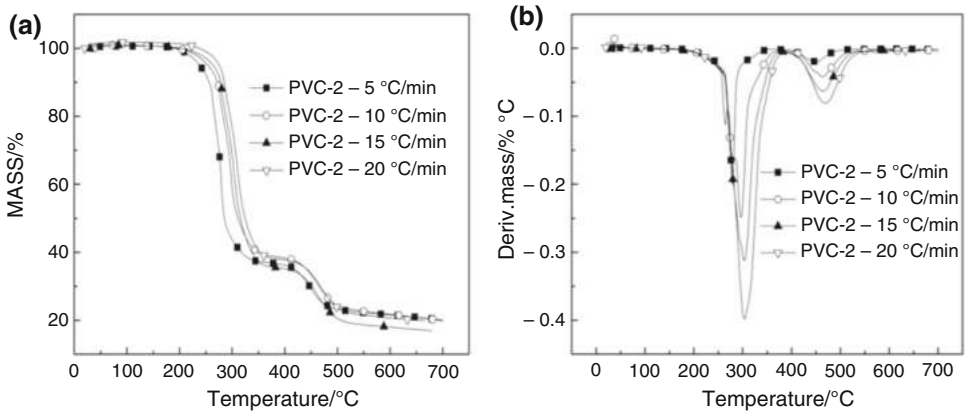

Fig. 8 TG (**a**) and DTG (**b**) curves of PVC–Sb_2O_3–TiO_2–SO_4^{2-} at different heating rates

mass loss. The first stage of mass loss in the temperature range of 200–380 °C was mainly the decomposition of PVC to remove HCl and DOP [29–32]. The residual char of PVC/Sb_2O_3 at different heating rates was higher than that of neat PVC, while the residual char of PVC/Sb_2O_3/(TiO_2/SO_4^{2-}) was much higher than that of neat PVC. The second mass loss stage beyond 400 °C was mainly caused by the cross-linking reaction after the formation of conjugate polyene cyclization after the removal of HCl, which was caused by the volatilization of aromatic hydrocarbon compounds [33]. It can be seen that the average residual char of PVC/Sb_2O_3 (17.5%) was 7% higher than that of neat PVC (10.5%). In addition, the average residual char of PVC/Sb_2O_3/(TiO_2/SO_4^{2-}) was 19.15%, and its residual char at different heating rates was higher than that of others, indicating that TiO_2/SO_4^{2-} solid superacid could catalyze early pyrolysis. The resulting char covered the surface of the PVC and insulated it from oxygen and heat. Therefore, combined with the LOI value, it can be inferred that the synergistic flame retardancy of TiO_2/SO_4^{2-} and Sb_2O_3 is good [34].

FTIR analysis of the residues heated to specific temperatures

PVC compounds were heated to 200, 300, 400, 500, 600, and 700 °C, respectively, and kept warm for 5 min in N_2 atmosphere. The thermal degradation products of PVC were analyzed by TGA-FTIR. Infrared spectra of neat PVC, PVC/Sb_2O_3, and PVC/Sb_2O_3/TiO_2/SO_4^{2-} are shown in Figs. 9–11.

PVC was characterized by an absorption peak at 619 cm^{-1}, which was attributed to the C–Cl stretching vibration [35]. It can be seen that several bands appeared at 1450–1675 cm^{-1}, which corresponded to the C=C stretching vibration of benzene ring skeleton and olefins.

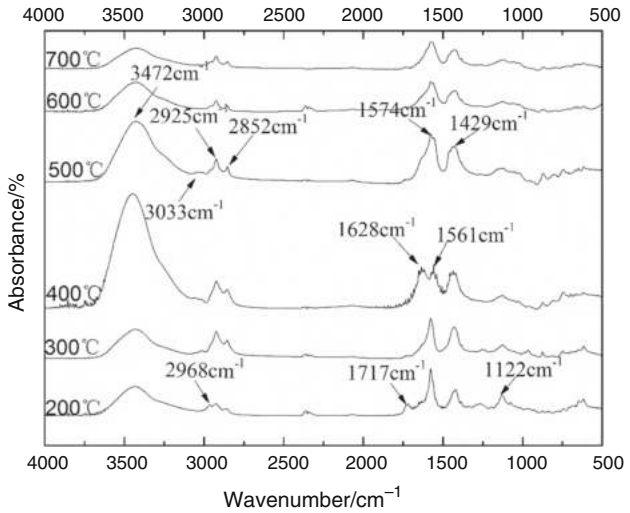

Fig. 9 Fourier-transform infrared (FTIR) spectra of the neat PVC specimens obtained at specific temperatures

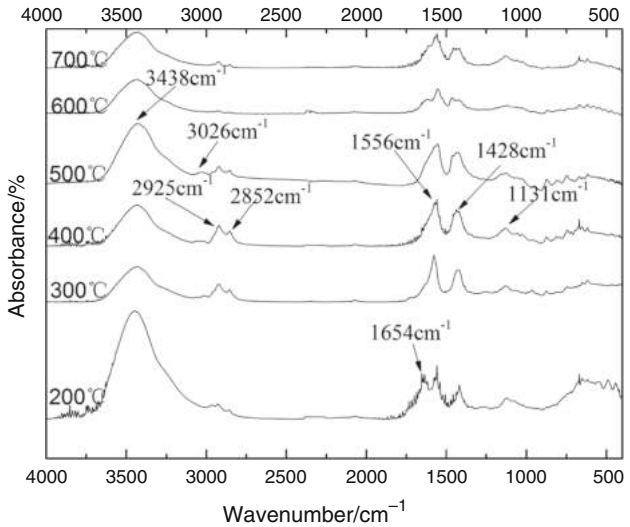

Fig. 10 Fourier-transform infrared (FTIR) spectra of the PVC–Sb_2O_3 specimens obtained at specific temperatures

The peak area of C=C initially increased, then decreased, and became stable at 600 °C. In addition, the appearance of the absorption peaks at around 1040–1311 cm^{-1} and 1717 cm^{-1} due to ester group and C=O bonds, respectively, could possibly be attributed to the presence of DOP [36]. As shown in Fig. 9, the disappearance of peaks at 1717 and 1260 cm^{-1} indicates decomposition. At the same time, the multiple peaks at 2968/2925/2852/1429 cm^{-1} corresponded to the stretching mode and flexural vibration of CH in CH_3 and CH_2. As the temperature increased, the peak intensity increased to a maximum at 400 °C and then the peak gradually disappeared. In Fig. 9, the band at

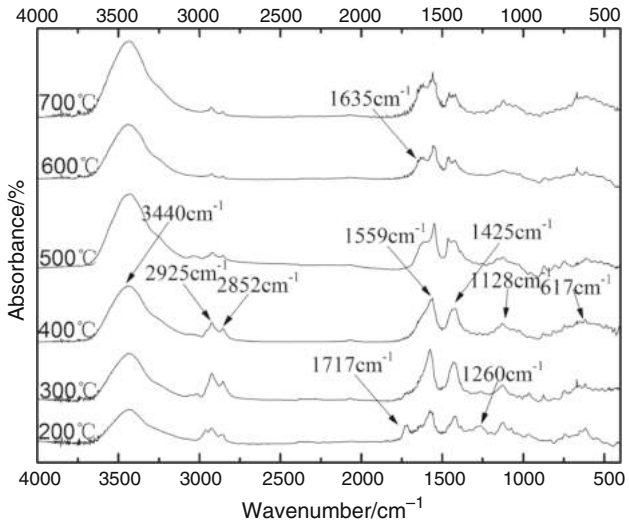

Fig. 11 Fourier-transform infrared (FTIR) spectra of the PVC–Sb_2O_3–(TiO_2–SO_4^{2-}) specimens obtained at specific temperatures

3432 cm^{-1} indicated O–H stretching vibration due to intermolecular hydrogen bonding [37].

According to the analysis of the data for neat PVC, several differences are observed in Figs. 10 and 11. The peaks for CH_2 and CH_3 of PVC/Sb_2O_3/TiO_2/SO_4^{2-} decreased soon, indicating that TiO_2/SO_4^{2-} prompted PVC to decompose early. In addition, as the temperature increased, the hydroxyl peak of PVC/Sb_2O_3 increased and then decreased, similar to neat PVC. However, the hydroxyl peak of PVC/Sb_2O_3/TiO_2/SO_4^{2-} did not decrease any further at 500 °C. Moreover, the C=C peak area of PVC/Sb_2O_3/TiO_2/SO_4^{2-} was larger than that of the other materials at 700 °C. To sum up, the results show that the hydroxyl group on the surface of carbon residue was very stable at high temperature. Therefore, high-temperature residual carbon mainly contained double bonds and hydroxyl groups. The influence of TiO_2/SO_4^{2-} on the early decomposition and stabilization of PVC is consistent with the TG results.

Scanning electron microscopy (SEM)

Figure 12 shows the SEM image of the char residue after burning of neat PVC. It can be seen that neat PVC itself had a certain ability to form char. However, the char layer structure lacked toughness, and charcoal layer itself was discontinuous. Thus, it could not effectively isolate oxygen and heat. Once the PVC was lit, heat and oxygen could freely enter and exit the PVC base material. Therefore, PVC is a flammable material and requires fire-retarding treatment.

Figure 13 presents the SEM image of char residue on the outer surface after combustion of PVC/Sb_2O_3.

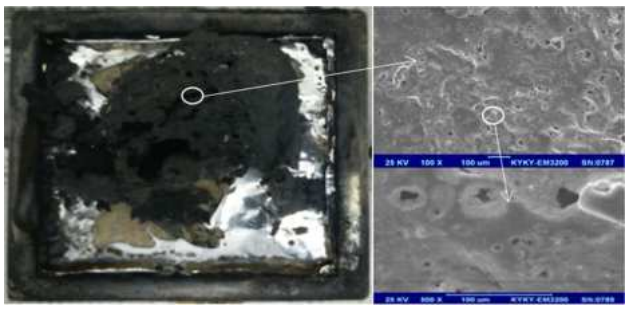

Fig. 12 SEM images of neat PVC composites

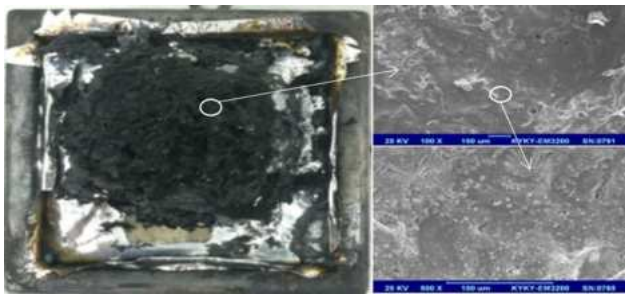

Fig. 13 SEM images of PVC–Sb_2O_3 composites

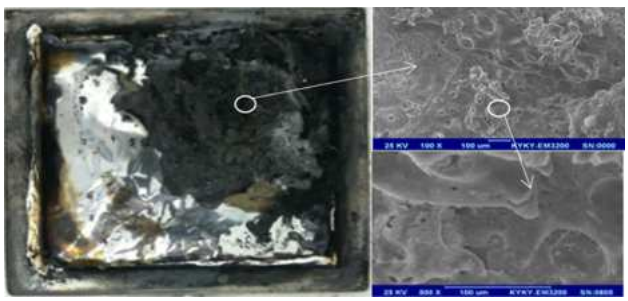

Fig. 14 SEM images of PVC–Sb_2O_3–(TiO_2–SO_4^{2-}) composites

Compared to Fig. 12, it can be seen that the char layer structure of PVC/Sb_2O_3 had considerable continuity and smoothness, and it was not easily broken. During the PVC combustion process, this char layer can effectively isolate oxygen and heat, protect the interior of the material, and delay the decomposition of PVC, which is very beneficial for the flame retardancy of PVC. Therefore, the flame retardant performance of PVC/Sb_2O_3 was improved.

Figure 14 shows the SEM images of PVC-3 composite. Compared with Fig. 12, it was observed that the surface of the char layer of PVC/Sb_2O_3/(TiO_2/SO_4^{2-}) had a continuous lamellar structure and the depth of the pores was also reduced compared to that of neat PVC. This structure was conducive to prevent the transfer of oxygen and heat and alleviate the thermal decomposition of PVC. Therefore, the flame retardant performance of the composite was superior to that of neat PVC. Compared with Fig. 13, it can be seen that the char of PVC/Sb_2O_3/(TiO_2/SO_4^{2-}) layer was not as smooth as that of the PVC/Sb_2O_3 but was tougher. Flammable gas cannot easily penetrate through such a barrier. Thus, PVC/Sb_2O_3/(TiO_2/SO_4^{2-}) had good flame retardant and smoke elimination properties.

Conclusions

In this work, a novel TiO_2/SO_4^{2-} solid superacid was successfully synthesized, which showed applicability as a flame retardancy synergist for PVC/Sb_2O_3 system. The PVC/Sb_2O_3/(TiO_2/SO_4^{2-}) composite was prepared by adding 6 phr solid superacid and Sb_2O_3 to PVC. The LOI value of neat PVC was only 23.6%, while that of the PVC/Sb_2O_3/(TiO_2/SO_4^{2-}) composite was 32.5%. In addition, the values of PHRR, THR, SPR, and TSP for PVC/Sb_2O_3/(TiO_2/SO_4^{2-}) were significantly reduced, compared to neat PVC. The above test results indicate that PVC had good flame retardant and smoke suppression performance upon the addition of TiO_2/SO_4^{2-}.

The thermal degradation of flexible PVC was studied in depth by TG in nitrogen atmosphere. The data for PVC/Sb_2O_3/(TiO_2/SO_4^{2-}) indicated increase in T_i, T_{max}, DTG peak value, Ea, and char residue compared to the corresponding values of neat PVC. Furthermore, from the analysis of char yield and SEM observation, the surface of the char layer of PVC/Sb_2O_3/(TiO_2/SO_4^{2-}) had a continuous lamellar structure and the depth of the pores was also reduced compared to neat PVC. Hence, superacid promoted the dehydration and cross-linking of PVC into charcoal and, together with Sb_2O_3, formed a continuous char layer. This layer could isolate oxygen and heat and effectively protect PVC. According to the TGA-FTIR analysis, high-temperature residual carbon mainly contained double bonds and hydroxyl groups. Moreover, TiO_2/SO_4^{2-} prompted the early decomposition and stabilization of PVC, which is consistent with the TG results. To sum up, excellent flame retardant performance was achieved through the synergistic effect between solid superacid and Sb_2O_3.

Therefore, this work demonstrated that the flame retardant property of PVC can be enhanced by using TiO_2/SO_4^{2-} solid superacid, which offers a promising solution for constructing high-efficiency flame-retardant polymer composites.

Funding Funding was provided by the Fundamental Research Funds for the National Natural Science Foundation (Grant No. 51574124) and the Central Universities (Grant No. 3142017065).

References

1. Starnes WH Jr. Structural and mechanistic aspects of the thermal degradation of poly(vinyl chloride). Prog Polym Sci. 2002;27:2133–70.
2. Xu J, Zhang C, Qu H, et al. Zinc hydroxystannate and zinc stannate as flame-retardant agents for flexible poly(vinyl chloride). J Appl Polym Sci. 2005;98(3):1469–75.
3. Tian CM, Wang H, Liu X, et al. Flame retardant flexible poly(-vinyl chloride) compound for cable application. J Appl Polym Sci. 2003;89(11):3137–42.
4. Coaker AW. Fire and flame retardants for PVC. J Vinyl Addit Technol. 2003;9:108–15.
5. Wei Q, Yang J, Zhang Y, Chang G, Du B. Determination of antimony (III) in environmental water samples in microemulsion system by the fluorescence quenching method. Talanta. 2002;58:419–26.
6. Oorts K, Smolders E, Degryse F, Buekers J, Gascó G, Cornelis G, Mertens J. Solubility and toxicity of antimony trioxide (Sb_2O_3) in soil. Environ Sci Technol. 2008;42:4378–83.
7. Pan Y, Wang D. One-step hydrothermal synthesis of nano zinc carbonate and its use as a promising substitute for antimony trioxide in flame retardant flexible poly(vinyl chloride). RSC Adv. 2015;5(35):27837–43.
8. Lu Y, Wu C, Xu S. Mechanical, thermal and flame retardant properties of magnesium hydroxide filled poly(vinyl chloride) composites: the effect of filler shape. Compos Part A. 2018;113:1–11.
9. Zhang B, Han J. Synthesis of microencapsulated zinc stannate and its application in flame-retardant poly(vinyl chloride) membrane material. Fire Mater Banner. 2018;42(1):109–18.
10. Pi H, Guo SY, Ning Y. Mechanochemical improvement of the flame-retardant and mechanical properties of zinc borate and zinc borate-aluminum trihydrate-filled poly(vinyl chloride). J Appl Polym Sci. 2003;89(3):753–62.
11. Ropero-Vega JL. Sulfated titania [TiO_2/SO_4^{2-}]: a very active solid acid catalyst for the esterification of free fatty acids with ethanol. Appl Catal A. 2010;379:24–9.
12. Zhang Z, et al. Thermal degradation behaviors and reaction mechanism of carbon fibreepoxy composite from hydrogen tank by TG-FTIR. J Hazard Mater. 2018;357:73–80.
13. Ding W, Li J, Tao K. Char strengthened by carbon microspheres formed in situ during combustion of IFR/EVA composites catalyzed by solid super acid. RSC Adv. 2014;4(64):34161.
14. Gao S, Ji Y, Zhang H, et al. Effects of modified zeolites by solid acid on flame retardant systems of polypropylene properties. Plastics. 2011;6:021.
15. Li Y, et al. Fatty acid methyl ester synthesis catalyzed by solid superacid catalyst SO_4^{2-}/ZrO_2-TiO_2/La^{3+}. Appl Energy. 2010;87(1):156–9.
16. Wang H, Jiang L, Wang Y, Zheng Y, Jiao X, Pan D. Synthesis of borneol from α-pinene catalyzed by SO_4^{2-}/TiO_2–La_3^+ nanometer rare-earth solid superacid. Inorg Nano-Met Chem. 2018;48(1):23–30. https://doi.org/10.1080/24701556.2017.1357622.
17. Ravi K, Krishnakumar B, Swaminathan M. Efficient, rapid, and solvent-free synthesis of substituted bis(indolyl)methanes using sulfated anatase titania as a solid acid catalyst. Synth React Inorg Met-Org Nano-Met Chem. 2015;45(9):1380–6.
18. Liao S, Donggen H, Denghua Yu, Yunlan S, Yuan G. Preparation and characterization of ZnO/TiO_2, SO_4^{2-}/ZnO/TiO_2 photocatalyst and their photocatalysis. J Photochem Photobiol A Chem. 2004;168:7–13.
19. Bickley R, Gonzalea-Carreno T, Lees J. A structural investigation of titanium dioxide photocatalysts. J Solid State Chem. 1991;92:178–90.
20. Gao M, Chen S, Wang H, Chai ZH. Design, preparation, and application of a novel, microencapsulated, intumescent, flame-retardant-based mimicking mussel. ACS Publ. 2018;3(6):6888–94.
21. Morgan AB, Bundy M. Cone calorimeter analysis of UL-94V-rated plastics. Fire Mater. 2007;31:257–83.
22. Kim J, Lee JH. Estimating the fire behavior of wood flooring using a cone calorimeter. J Therm Anal Calorim. 2012;110:677–83.
23. Han L, et al. Metallic ferrites as flame retardants and smoke suppressants in flexible poly(vinyl chloride). Therm Anal Calorim. 2016;123(1):293–300.
24. Fang Y, Wang Q, Bai X, Wang W, Cooper PA. Thermal and burning properties of wood flour-poly(vinyl chloride) composite. J Therm Anal Calorim. 2012;109:1577–85.
25. Ming G, Li J, Zhang X, Yue L, Chai Z. The flame retardancy of epoxy resin including the modified graphene oxide and ammonium polyphosphate. Combust Sci Technol. 2018;190(6):1126–40.
26. Dong M, Gu X, Zhang S, et al. Effects of acidic sites in HA zeolite on the fire performance of polystyrene composite. Ind Eng Chem Res. 2013;52(26):9145–54.
27. Kissinger HE. Variation of peak temperature with heating rate in differential thermal analysis. J Res Natl Bur Stand. 1956;57(4):217–21.
28. Sun Y, et al. Thermal behavior of the flexible polyvinyl chloride including montmorillonite modified with iron oxide as flame retardant. J Therm Anal Calorim. 2018;131:65–70.
29. Chunming T, Hai W, Xiulan L. Flame retardant flexible poly(-vinyl chloride) compound for cable application. J Appl Polym Sci. 2003;89(11):3137–42.
30. Ning T, Guo SY. Flame-retardant and smoke-suppressant properties of zinc borate and aluminum trihydrate filled rigid PVC. J Appl Polym Sci. 2000;77(14):3119–27.
31. Gumargalieva KZ. Problems of ageing and stabilization of poly(vinyl chloride). Polym Degrad Stab. 1996;52(1):73–9.
32. Tian CM, Wang H, Guo HZ. Low-melting sulfate glasses as additives to semirigid PVC and their flame retardant and smoke suppressant properties. J Vinyl Addit Technol. 2003;9(2):69–80.
33. Knumann R, Bockhorn H. Investigation of the kinetics of pyrolysis of PVC by TG-MS-analysis. Combust Sci Technol. 1994;101(1):285–99.
34. Gao T, et al. Preparation of zinc hydroxystannate-decorated graphene oxide nanohybrids and their synergistic reinforcement on reducing fire hazards of flexible poly(vinyl chloride). Nanoscale Res Lett. 2016;11:192.
35. Wang X, Zhang Q. Effect of hydrotalcite on the thermal stability, mechanical properties, rheology and flame retardance of poly(-vinyl chloride). Polym Int. 2004;53(6):698–707.
36. Qi Y, Wu W, Han L, Qu H, Han X, Wang A, Xu J. Using TG-FTIR and XPS to understand thermal degradation and flame-retardant mechanism of flexible poly(vinyl chloride) filled with metallic ferrites. J Therm Anal Calorim. 2015;123(2):1263–71.
37. Zheng L, Qiao Z, Xu X, Wang L. Effects of γ irradiation on the compression and inter-laminar shear properties of G10 for the BESIII beam pipe supporting flange. Fusion Eng Des. 2017;117:24–9.